Global Change Biology

Global Change Biology (2010) **16**, 2024–2038, doi: 10.1111/j.1365-2486.2009.02156.x

Nitrogen deposition in tropical forests from savanna and deforestation fires

YANG CHEN*, JAMES T. RANDERSON*, GUIDO R. VAN DER WERF†, DOUGLAS C. MORTON‡, MINGQUAN MU* and PRASAD S. KASIBHATLA§

*Department of Earth System Science, University of California, Irvine, CA 92697, USA, †Faculty of Earth and Life Sciences, VU University, 1081HV Amsterdam, The Netherlands, ‡NASA Goddard Space Flight Center, Biospheric Sciences Branch, Code 614.4, Greenbelt, MD 20771, USA, §Nicholas School of the Environment, Duke University, Durham, NC 27708, USA

Abstract

We used satellite-derived estimates of global fire emissions and a chemical transport model to estimate atmospheric nitrogen (N) fluxes from savanna and deforestation fires in tropical ecosystems. N emissions and reactive N deposition led to a net transport of N equatorward, from savannas and areas undergoing deforestation to tropical forests. Deposition of fire-emitted N in savannas was only 26% of emissions – indicating a net export from this biome. On average, net N loss from fires (the sum of emissions and deposition) was equivalent to approximately 22% of biological N fixation (BNF) in savannas (4.0 kg N ha^{-1} yr^{-1}) and 38% of BNF in ecosystems at the deforestation frontier (9.3 kg N ha^{-1} yr^{-1}). Net N gains from fires occurred in interior tropical forests at a rate equivalent to 3% of their BNF (0.8 kg N ha^{-1} yr^{-1}). This percentage was highest for African tropical forests in the Congo Basin (15%; 3.4 kg N ha^{-1} yr^{-1}) owing to equatorward transport from frequently burning savannas north and south of the basin. These results provide evidence for cross-biome atmospheric fluxes of N that may help to sustain productivity in some tropical forest ecosystems on millennial timescales. Anthropogenic fires associated with slash and burn agriculture and deforestation in the southern part of the Amazon Basin and across Southeast Asia have substantially increased N deposition in these regions in recent decades and may contribute to increased rates of carbon accumulation in secondary forests and other N-limited ecosystems.

Keywords: atmospheric transport, biomass burning, global carbon cycle, Hadley circulation, nitrogen limitation, pyrodenitrification

Received 11 June 2009; revised version received 30 November 2009 and accepted 4 December 2009

Introduction

Nitrogen (N) is an essential element in Earth's atmosphere, biosphere, and hydrosphere (Galloway *et al*., 2003). The vast majority of N in the atmosphere is N_2, which is biologically unavailable to most organisms. N must be converted from N_2 to reactive N (N_r), which includes inorganic oxidized forms (e.g., NO, NO_2, and HNO_3), inorganic reduced forms (NH_3 and NH_4^+), and organic forms (e.g., amino acids and urea), before its use by microbes or plants. N_2 to N_r conversion (N fixation) occurs during electrical discharges in lightning and by some bacteria and algae via a process known as biological N fixation (BNF) (Cleveland *et al*., 1999). In terrestrial ecosystems, humans have more than doubled the flux of N_2 to N_r through fossil fuel use, industrial N fertilizer production, and cultivation of N-fixing crops (Vitousek *et al*., 1997; Smil, 1999; Galloway *et al*., 2004, 2008).

Much of our knowledge of the N cycle and the consequences of N enrichment comes from studies of temperate ecosystems, where industrial and agricultural modification of N availability has been substantial. Tropical ecosystems respond differently to perturbations in N cycling (Matson *et al*., 1999; Davidson *et al*., 2004; Bustamante *et al*., 2006) and important uncertainties remain with respect to our understanding of N deposition, fixation, and loss pathways in these ecosystems. With implementation of stricter air quality standards, N emissions and deposition are likely to decrease in temperate regions, particularly in developed countries. In contrast, N emissions and deposition in tropical and subtropical regions are likely to increase (Galloway *et al*., 1994; Lamarque *et al*., 2005; Dentener *et al*., 2006). Since tropical forests and savannas account for more than half of global terrestrial net primary production (NPP) (Field *et al*., 1998) and may contribute substantially to contemporary (Stephens *et al*., 2007) and future land C sinks (Friedlingstein *et al*., 2006), it is important to quantify the processes contributing to changing levels of N deposition in these ecosystems and subsequent impacts on N cycling and carbon storage.

Fires, including wildfires and prescribed fires, influence the N cycle within tropical ecosystems by changing both the availability and the mobility of N. Fire-induced losses of N by means of volatilization are

Correspondence: Yang Chen, tel. + 1 949 824 0597, e-mail: yang.chen@uci.edu

substantial (Raison *et al*., 1985; Cook, 1994; Bustamante *et al*., 2006) and contribute to wet and dry deposition of N in downwind ecosystems. Nitric oxide (NO) and ammonia (NH_3) are the primary N_r gases emitted from these fires, accounting typically for over 90% of N_r emissions (Andreae & Merlet, 2001). These gases are converted to other N_r gases and to particulate species (NO_3^-, NH_4^+, and organic aerosols) by means of multiple reaction pathways (Crutzen & Andreae, 1990; Atkinson, 2000). The ultimate fate of N_r in the atmosphere is removal by wet and dry deposition – processes regulated by the amount and intensity of precipitation, surface roughness, wind speed, and regional patterns of atmospheric transport (Dentener *et al*., 2006). Emissions of N_r probably account for only 40%–50% of the N present in fuels before combustion, as some is retained within the ecosystem in combusted residues (approximately 20%) and the remainder (another 30%–40%) is transformed directly into N_2 during combustion (Lobert *et al*., 1990; Kuhlbusch *et al*., 1991). N_2 emissions from fires represent a net loss of N from the biosphere – contrasting with N_r fluxes that instead lead to redistribution of N_r across different ecosystems.

Fires influence nutrient cycling in tropical ecosystems in multiple ways, apart from the emissions during the initial event and subsequent deposition of the reactive component described above. Immediately after fire, soil NO and N_2O losses often increase for relatively short periods (Verchot *et al*., 2006; Davidson *et al*., 2008), probably from N additions in ash to the soil surface and mortality of fine roots that increase levels of mineralization and nitrification (Dunn *et al*., 1979; Neff *et al*., 1995). Yienger & Levy (1995) incorporated these responses into a global model, and estimated that postfire pulses of NO account for approximately 10% ($0.6\,Tg\,N\,yr^{-1}$) of tropical soil emissions annually. Over a period of years to decades, fire-induced changes in species composition (e.g., Scholes & Archer, 1997) can alter N cycling by several different pathways, including by changing the abundance of N-fixing trees and shrubs (Okello *et al*., 2008), by changing the abundance of asymbiotic N fixers (Mack *et al*., 2001), or by triggering a series of feedbacks that change the long-term fire regime (Mack & D'Antonio, 1998; Cochrane *et al*., 1999; Hoffmann *et al*., 2002) and thus the volatilization losses described above. In many grassland and savanna ecosystems, grazing intensity plays an important role in regulating N losses during fire (Hobbs *et al*., 1991) and N limitation in postfire ecosystems (Buis *et al*., 2009).

Deposition of N from tropical fires is likely to have spatially heterogeneous effects on NPP, depending in part on ecosystem type, soil properties, past disturbance history, and N inputs from other sources. Multiple studies and meta-analyses document widespread N limitation in savanna and grassland ecosystems (Elser *et al*., 2007; Lebauer & Treseder, 2008; Xia & Wan, 2008), with the magnitude of sensitivity often modulated by grazing intensity and fire frequency (Cech *et al*., 2008). Patterns in tropical forests are more complex, but may allow for several generalizations. First, in many but not all fertilization studies in secondary forests, N limits multiple components of NPP (Campo & Vázquez-Yanes, 2004; Davidson *et al*., 2004). Postdisturbance trajectories of litter and soil chemical composition and N_2O fluxes provide additional indirect evidence that N limitation is strong during early stages of secondary succession (Davidson *et al*., 2007). N is also limiting in forests on relatively young and unweathered soils (Vitousek & Farrington, 1997; Harrington *et al*., 2001). In contrast, in primary tropical forests on highly weathered soils, phosphorus (P) limits NPP and in many instances fertilization by N alone does not stimulate significant increases in production (Harrington *et al*., 2001). However, stimulation of some NPP components by N has been observed in a lowland forest, including increases in the reproductive fraction of litterfall (Kaspari *et al*., 2008). Further, other studies in lowland forests document N by P interactions, in which the combined response to the two nutrients exceeds the response to P alone (Tanner *et al*., 1992; Mirmanto *et al*., 1999; Harrington *et al*., 2001). In the broader context of atmospheric deposition from many sources, including P from fires, dust, and biogenic sources (Mahowald *et al*., 2008), this suggests that N deposition from fire has the potential to synergistically interact with other deposition elements to sustain productivity.

Here we assessed the spatial and temporal patterns of N emissions and N_r deposition caused by fires in tropical ecosystems. We estimated fire emissions using the Global Fire Emission Database version 2 (GFEDv2; van der Werf *et al*., 2006), which combines satellite observations of burned area (BA) (Giglio *et al*., 2006) with estimates of fuel loads (FL) obtained from a biogeochemical model constrained by other satellite data. We estimated pyrodenitrification losses to N_2 for different ecosystems by scaling up measurements obtained from chamber combustion experiments (Kuhlbusch *et al*., 1991). Transport and deposition of N_r were simulated using the GEOS-Chem global chemical transport model (CTM) (Bey *et al*., 2001). We performed 10-year (1997–2006) global-scale simulations, focusing our analysis and discussion on tropical ecosystems. We partly validated our modeled fluxes by comparing our results with published observations of N deposition. By quantifying the net N balance associated with both emissions and deposition in each model grid cell, we assessed the spatial distribution of donor and recipient regions. Emissions and deposition

fluxes were compared with terrestrial and marine BNF fluxes (Cleveland *et al*., 1999; Deutsch *et al*., 2001; Lee *et al*., 2002) as a means to gauge the relative impact of fires on ecosystem N cycling.

Materials and methods

N_r emissions from biomass burning

The GFEDv2 product consists of $1^\circ \times 1^\circ$ gridded monthly BA, FL, combustion completeness (CC), emission factors (EMFs), and emissions (E) for different gas and aerosol species (van der Werf *et al*., 2006). BA was derived using Moderate Resolution Imaging Spectroradiometer (MODIS) active fire and BA datasets for the 2000–2006 period as described by Giglio *et al*. (2006). BA estimates were extrapolated back in time using Tropical Rain Monitoring Mission and Along Track Scanning Radiometer active fire observations. FL and CC values were estimated using the Carnegie–Ames–Stanford Approach (CASA) biogeochemical model constrained by additional satellite observations of fractional tree cover and the fraction of absorbed photosynthetically active radiation by plant canopies (van der Werf *et al*., 2006). Emission rates for each gaseous N species were calculated by applying EMFs to fire-emitted carbon fluxes from CASA

$$E = EMF \times BA \times FL \times CC. \quad (1)$$

Organic dry matter (DM) in the fuel was assumed to be comprised of 45% carbon. EMFs, defined as the emission of species (g) per 1 kg burned DM, were obtained from Andreae & Merlet (2001) with updates from M. Andreae (personal communication).

Comparison with atmospheric carbon monoxide (CO) observations provides some validation of our carbon emissions and CTM. GFEDv2 CO emissions in equatorial Asia, for example, required a small negative adjustment (from 0% to 22% depending on atmospheric inversion approach) to match Measurements of Pollution in the Troposphere (MOPITT) satellite observations during 2000–2006 (van der Werf *et al*., 2008).

Atmospheric CO anomalies, obtained after removing an annual mean cycle and long-term trend, have large variations from year-to-year that are primarily driven by fires (e.g., van der Werf *et al*., 2004). This is because, at remote flask sampling stations in both hemispheres, other important CO sources such as methane and volatile organic compound oxidation and fossil fuel emissions vary by only a small amount from year-to-year. In contrast, fires on different continents may vary by a factor of 30 or more (e.g., van der Werf *et al*., 2008) as a consequence of year-to-year changes in climate and patterns of land use. CO anomalies from GFEDv2 in the GEOS-CHEM model had a mean correlation (r) of 0.78 with observations from NOAA Global Monitoring Division (GMD) stations in the northern hemisphere (NH) and 0.67 with GMD stations in the southern hemisphere (SH) during 1997–2008 (Table 1; Fig. S1 in supporting information). Similarly, the ratio of modeled to observed standard deviations of CO anomalies from GMD was 0.92 and 1.01, respectively, for NH and SHs. These results suggest that while important uncertainties still remain in our emissions and transport estimates, these two model components are probably adequate for preliminary assessments of the impact of fires on atmospheric chemistry.

N_r can be emitted into the atmosphere in different chemical forms and physical phases. NO_x and NH_3 account for the majority (>90%) of N_r emissions from biomass burning (Andreae & Merlet, 2001). In our model simulations and calculations, we used the sum of gaseous NO_x and NH_3 emissions to represent total N_r emissions from biomass burning. The low bias we expected from neglecting the remaining N_r emissions (e.g., N_2O, HCN, and acetonitrile) was small compared with uncertainties associated with BA (e.g., Giglio *et al*., 2006), FL, CC, and NO and NH_3 EMFs.

Table 1 Comparison of monthly mean CO anomalies from NOAA Global Monitoring Division (GMD) measurements (during 1997–2008) with CO anomalies from the GEOS-Chem chemical transport model using GFEDv2 biomass burning emissions

Latitude	Number of stations	Stations	Correlation coefficient	$\sigma_{mod}/\sigma_{obs}$
70°N–90°N	3	ALT, ZEP, BRW	0.83	1.08
50°N–70°N	6	STM, ICE, BAL, CBA, MHD, SHM	0.80	1.11
30°N–50°N	13	HUN, LEF, UUM, BSC, NWR, UTA, AZR, TAP, WLG, BME, BMW, WIS, POCN30,	0.71	0.83
10°N–30°N	12	IZO, MID, KEY, ASK, MLO, KUM, GMI, RPB, POCN25, POCN20, POCN15, POCN10	0.85	0.72
10°S–10°N	7	CHR, SEY, ASC, POCN05, POC000, POCS05, POCS10	0.67	0.84
30°S–10°S	6	SMO, EIC, POCS15, POCS20, POCS25, POCS30	0.72	0.85
50°S–30°S	2	CGO, CRZ	0.59	1.16
70°S–50°S	3	TDF, PSA, SYO	0.69	1.07
90°S–70°S	2	HBA, SPO	0.66	1.03

The model results were sampled at the time and place of the measurements. σ is the standard deviation of modeled or measured CO anomalies during this period. To estimate CO anomalies, both an annual cycle and a linear trend were removed from the observations and model estimates at each station using the same procedure. NOAA GMD CO observations were analyzed following the approach described by Novelli *et al*., (1998).

Direct emissions of N_2 during biomass burning

A large gap has been observed in the N balance between its content in the fuel and the sum of measured N in gaseous emissions and what remains after combustion in the ash (Lobert *et al*., 1990). By burning different biomass materials in a stainless steel chamber, Kuhlbusch *et al*. (1991) showed that the missing N is mostly molecular N (N_2), which accounts for approximately one third of fuel N. This experiment also showed that N_2 is formed primarily during the flaming stage and thus the total amount of N_2 production (as a fraction of fuel N) depends on fire intensity. The CO to CO_2 emission ratio serves as an indicator for the relative extent of flaming combustion and may serve as a means to scale fire intensity estimates over larger regions. Analysis of the Kuhlbusch *et al*. (1991) measurements showed that the N_2–N to N_r–N ratio of fire emissions was inversely related to its CO/CO_2 ratio (Fig. S2).

The N_2–N to N_r–N ratio derived from this relationship was used to estimate global N_2 emissions from biomass burning. In this study, we estimated the CO/CO_2 ratio for three different fire types: savanna and grassland fires, tropical forest fires, and extratropical forest fires using the EMFs of CO and CO_2 listed in Table 1 of Andreae & Merlet (2001). A 2°(latitude) $\times$ 2.5° (longitude) vegetation map of these three types (Andreae & Merlet, 2001) was used to derive the global gridded N_2–N to N_r–N ratio. For each grid cell, we scaled GFED N_r emissions by this ratio to obtain the fire emissions rate of N_2.

Model simulations of N transport and deposition

We used the GEOS-Chem model to calculate the transport, transformation, and deposition of biomass burning emitted N species. GEOS-Chem is a global 3-D CTM (Bey *et al*., 2001) driven by assimilated meteorological observations from the Goddard Earth Observing System (GEOS) of the NASA Global Modeling and Assimilation Office (GMAO). In this study, we used version 08-01-01 of the model with $2^\circ \times 2.5^\circ$ horizontal resolution and 30 vertical layers between the surface and 0.01 hPa.

The GEOS-Chem model includes a detailed description of tropospheric O_3–NO_x–hydrocarbon chemistry (Wang *et al*., 1998). Emission sources of N include NO_x from lightning, soil and fertilizer, aircraft, biofuel, fossil fuel, biomass burning, and NH_3 from biofuel, fossil fuel, biomass burning, and natural sources (e.g., soils, vegetation, and wild animals). N tracers are present in gas phase [e.g., NO_x, peroxyacyl nitrate (PAN), HNO_3, N_2O_5, and NH_3] or aerosol phase (NH_4^+, N on sulfate, and N on sea salt). These tracers are transported by meteorology-driven advection and convection processes, and are removed by the action of precipitation (wet deposition) or by interaction with vegetation or soils in the lowest atmospheric layer (dry deposition) or vegetation (dry deposition).

We performed GEOS-Chem full chemistry simulations over a 10-year period (1997–2006) using the GFEDv2 inventory, which resolves the interannual variability of biomass burning emissions. N emissions from other sources were obtained from climatological inventories which represent contemporary (circa 2000) emissions. After a 3-month spin-up period with the same initial conditions, two sets of simulations were conducted: one with biomass burning emissions prescribed from GFEDv2, and another without these emissions. The difference between these two simulations represents the effect of biomass burning emissions on N transport and deposition. We recorded monthly mean deposition rates for each N species through dry and wet deposition. Wet deposition included convective and large-scale components (Liu *et al*., 2001). Total deposition rate of N from biomass burning was then calculated for each $2^\circ \times 2.5^\circ$ model grid cell.

BNF

Cleveland *et al*. (1999) reviewed published studies and generated three linear regressions (conservative, central, and upper-bound) between BNF and evapotranspiration (ET) in terrestrial ecosystems. Galloway *et al*. (2004) argued that contemporary N fixation rates are at the lower end of this range, due to sampling biases in many plot-scale studies. In this study, as a simple measure to gauge the relative importance of fire impacts on ecosystem N fluxes, we constructed maps of BNF using the mean of central and conservative regressions between BNF and ET from Cleveland *et al*. (1999). The global ET estimates we used for this spatial extrapolation were developed using satellite data and a bio-meteorological approach by Fisher *et al*. (2008). The spatial pattern of BNF, as well as probability distributions of ET and BNF across tropical terrestrial ecosystems, are shown in Fig. 1. Based on the distribution of ET in savanna and tropical forest areas, we estimated the mean BNF rates in these two biomes to be 18.6 and 26.2 kg N ha^{-1} yr^{-1} (Fig. 1), respectively. As expected, these globally extrapolated BNF values were similar to mean estimates from Cleveland *et al*. (1999).

Previous estimates of global ocean BNF range from 60 to 200 Tg N yr^{-1} (Duce *et al*., 2008). Large uncertainty remains in the estimation of regional marine N fixation (Mahaffey *et al*., 2005). In this study, we used reported estimates of BNF rates for the tropical Atlantic (Lee *et al*., 2002) and Pacific (Deutsch *et al*., 2001). Owing to a dearth of data for other regions, we assumed that the mean of these two rates represented the N fixation rate in other tropical oceans.

Results

Validation of wet and dry deposition

Relative to NH industrial regions, few N deposition measurements exist for tropical land and ocean regions. Here we compiled wet and dry N deposition measurements in tropical regions published in recent years. We only considered observations from 1996 to 2006 to ensure overlap with the period of our satellite-derived fire emissions time series. We differentiated urban and nonurban observations according to the description of the site in the original literature or the proximity of the measurement station to an urban center. Based on the original data, we calculated wet and dry deposition

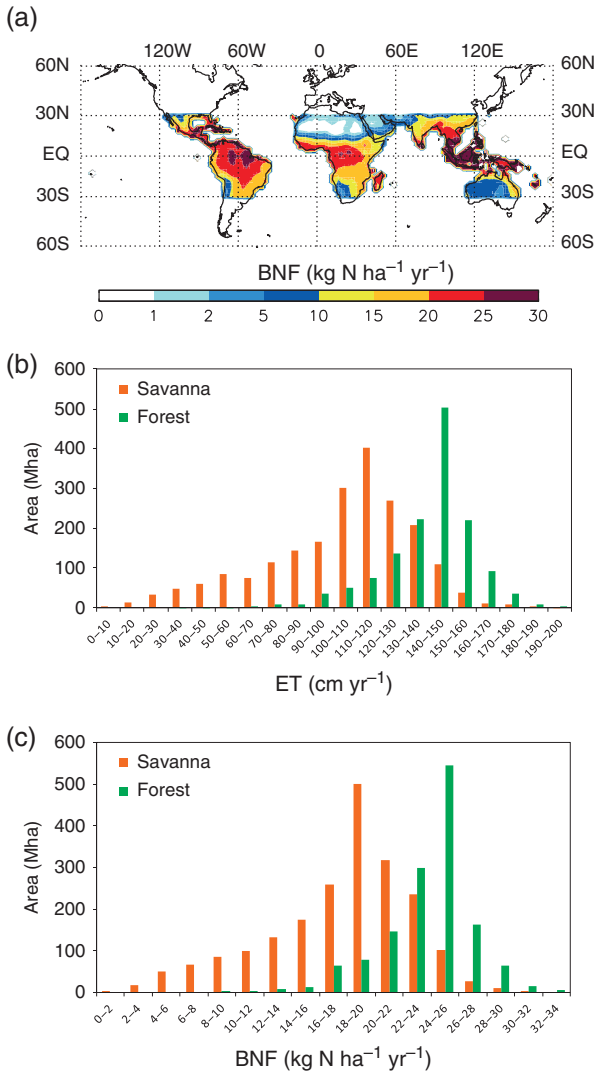

Fig. 1 (a) The spatial distribution of biological nitrogen fixation (BNF) in tropical ecosystems derived using regression estimates from Cleveland *et al.* (1999) and evapotranspiration (ET) maps from Fisher *et al.* (2008). (b) The distribution of evapotranspiration in savanna and tropical forest ecosystems from Fisher *et al.* (2008). (c) The distribution of BNF in savanna and tropical forests as a function of area.

rates for total oxidized N (NO_3–N) and reduced N (NH_4–N) with units of kg N ha^{-1} yr^{-1}. Altogether, we reported wet and dry deposition rates from 26 nonurban stations. The location and time period of these measurements, as well as observed and modeled deposition rates, are summarized in Table S1. We compared these observations with modeled deposition fluxes, which were sampled in grid cells corresponding to observations during the month when observations were available. For locations that had measurements only during 1996, we compared the deposition rates with our 10-year (1997–2006) mean model results.

Overall, the model simulation corresponded reasonably well to wet and dry deposition observations at nonurban sites (Fig. 2). About 75% of the wet deposition rates and 80% of the dry deposition rates agreed within $\pm$ 50% of the observations. This agreement was similar to previous comparisons of N deposition between models and observations (Lamarque *et al.*, 2005; Dentener *et al.*, 2006). The model somewhat underestimated NO_3–N wet deposition and overestimated NH_4–N dry deposition. Simulations were more strongly correlated with measurements for dry deposition than for wet deposition, as indicated by the r values shown in Fig. 2. For sites substantially affected by fire emissions (filled points in Fig. 2), the agreement between our model simulation and measurements was similar.

In contrast to nonurban sites, the model was generally biased low for urban data, which were likely affected by nearby fossil fuel emissions (Fig. 2). Urban data were generally not representative of the coarse $2^\circ \times 2.5^\circ$ grid cells in the model, so they were not included in our linear regressions. Most of these urban measurement sites were located in Southeast Asia.

Gross N emissions from fires

Emissions of N_r and N_2 by fires were 11.4 Tg N yr^{-1} (5.4 kg N ha^{-1} yr^{-1}) in savannas and 5.3 Tg N yr^{-1} (3.8 kg N ha^{-1} yr^{-1}) in tropical forests, with these two biomes accounting for 75% of global fire N emissions (Fig. 3a and Table 2). High emission rates occurred in African savannas, as well as in deforestation regions in South America and Southeast Asia (see Fig. S3). Losses directly to N_2 accounted for about half of the total N emissions flux. This fraction was slightly higher for savannas than for tropical forests because of more complete combustion (Fig. S2).

N deposition rates from biomass burning

Fires contributed substantially to both N emissions and deposition in the tropics compared with other natural and anthropogenic components (Fig. 4). Deposition rates from fires were highest near source regions – with maxima on the perimeter of the Congo basin in Africa (up to 9.9 kg N ha^{-1} yr^{-1}), in southern Borneo in equatorial Asia (up to 9.7 kg N ha^{-1} yr^{-1}), and across the Brazilian state of Mato Grosso, eastern Bolivia, and Paraguay in South America (up to 5.3 kg N ha^{-1} yr^{-1}) (Fig. 3b). In these areas, fires accounted for between 50% and 80% of the total N deposition flux – considering all other natural and anthropogenic sources. These results implied that unburned forest and savanna ecosystems in these regions (including parks and other protected

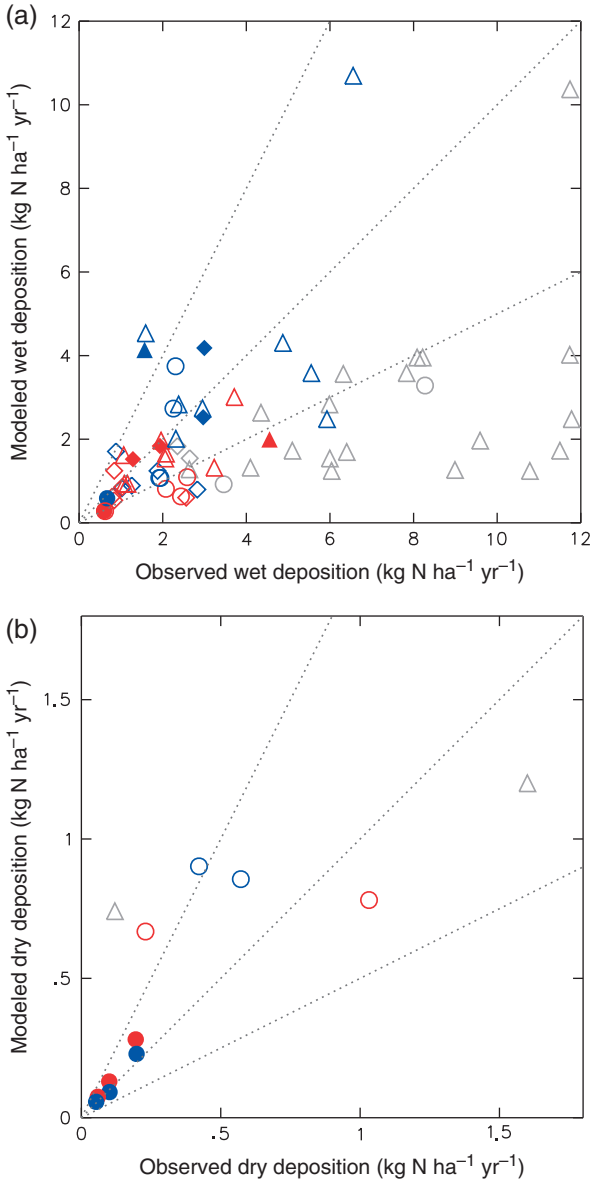

Fig. 2 Comparison of observed and modeled (a) wet and (b) dry N deposition rates (kg N ha^{-1} yr^{-1}) in tropical regions, with NO_3-N points in red and NH_4-N points in blue. Gray points are observation stations near urban areas. Circles, diamonds, and triangles represent data from South America, Africa, and Southeast Asia, respectively. Dashed lines indicate 1:1, 1:2, and 2:1 relationships. Filled points represent a subset of nonurban stations where more than 30% of the annual N deposition originated from fires. Wet and dry deposition comparisons had similar regression statistics (wet deposition had a slope of 1.01, an intercept of −0.34, 42 points, $r = 0.89$, and $P < 0.01$ whereas dry deposition had a slope of 0.84, an intercept of −0.08, 10 points, $r = 0.84$, and $P < 0.01$). For stations where fire deposition was significant, the linear fits of wet deposition had a slope of 0.64, an intercept of −0.41, eight points, $r = 0.74$, and $P \approx 0.02$ whereas dry deposition had a slope of 1.36, an intercept of −0.02, six points, $r = 0.94$, and $P < 0.01$.

areas) experienced relatively high levels of N deposition from nearby savanna and deforestation fires.

Seasonal variations in N deposition were closely linked with the timing of fire emissions (Fig. 5). Total wet deposition was comparable to total dry deposition across the tropics, although regionally the relative importance of these two pathways varied. Wet deposition accounted for a larger fraction of total deposition in Southeast Asia (57%) and NH Africa (55%) than in South America (46%) or Southern Hemisphere (SH) Africa (39%). About 2/3 of the total N wet deposition occurred in the gas phase (NH_3 and HNO_3). The relative importance of wet deposition as an atmospheric loss pathway increased toward the end of the fire season on all three continents (Fig. 5), as a consequence of increasing precipitation levels. Model estimates of the total deposition rate for oxidized N and reduced N were similar. Separation of N deposition by its oxidation form is important for assessing N deposition effects on ecosystem function. Reduced N, for example, can reduce base cation uptake by plants (de Graaf *et al.*, 1998), causing changes in species composition in ecosystems such as heathlands (van den Berg *et al.*, 2008) and peatlands (Paulissen *et al.*, 2004).

Changes in N surface budgets caused by fire emissions

The emissions and deposition of N from fires led to a net loss of N from the terrestrial biosphere and a redistribution of N among ecosystems. Savanna ecosystems in Africa and South America and tropical deforestation frontiers in all three regions experienced a net loss of N (Figs. 3c, S2). Net gains at a regional scale occurred in interior tropical forests and over tropical oceans.

The net loss of N (N_r and N_2) from savanna ecosystems was largest in Africa (Table 2), where fires burned more frequently than on other continents (Giglio *et al.*, 2006). Net fire losses were equal to approximately 34% of BNF in savanna ecosystems in Africa, corresponding to 6.7 Tg N yr^{-1} or 5.7 kg N ha^{-1} yr^{-1} in savanna ecosystems (Tables 2, S2). Deposition from fires in African savannas offset only 26% of emissions to N_2 and N_r (Table 2). Considering N_r, deposition from fires was only 53% of emissions, indicating that African savannas were a net exporter of N_r to other biomes, including tropical forests in the Congo basin and the tropical Atlantic Ocean (Fig. 3b). For savannas across all three continents, net fire N losses were equal to 22% of BNF (4.0 kg N ha^{-1} yr^{-1}), with only 55% of N_r emissions offset by deposition inputs.

Tropical forests received large N deposition inputs from savanna fires but also lost N through deforestation fires. Overall, tropical forest fires had a net N loss equal to approximately 8% of BNF (2.8 Tg N yr^{-1} or

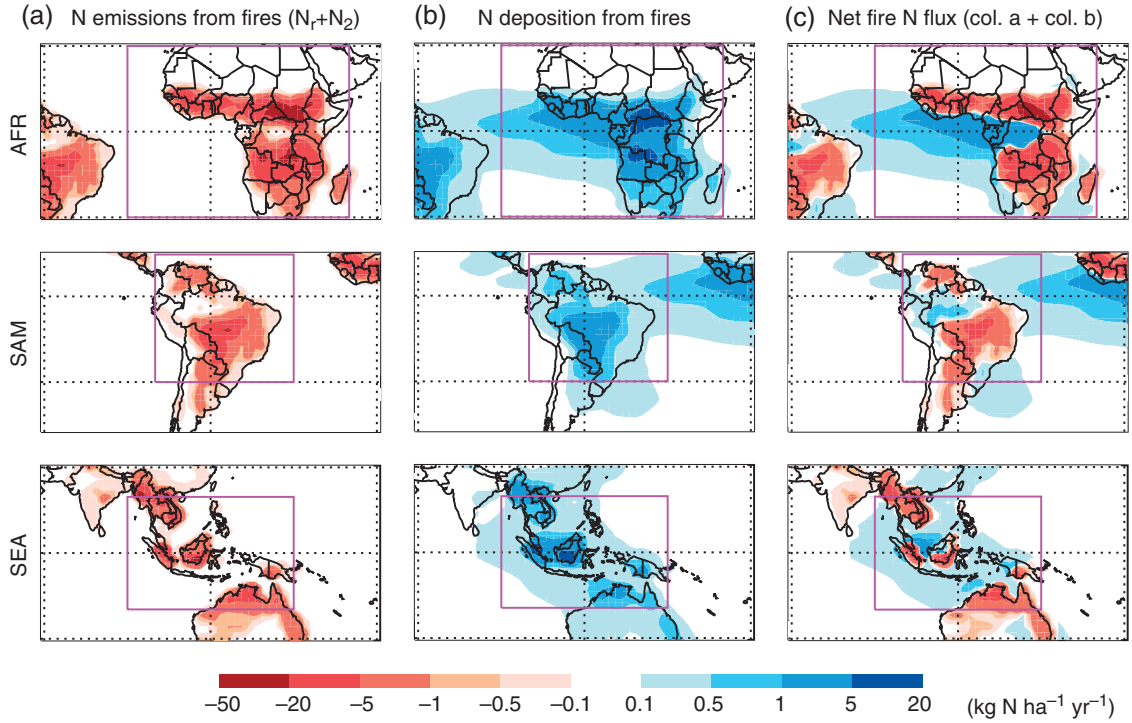

Fig. 3 Simulated 10-year average (a) N emissions from fires [the sum of reactive N (N_r) and N_2], (b) N deposition from fires, and (c) net fire N flux with respect to the surface. The net fire N flux includes both losses from N_r and N_2 emissions and gains from N deposition (the sum of column a and b). The values are in kg N ha^{-1} yr^{-1}. Blue and red colors represent N addition to and loss from terrestrial ecosystems, respectively. Solid pink boxes define the domains of tropical Africa (AFR), tropical South America (SAM), and tropical Southeast Asia (SEA) used in the text.

2.0 kg N ha^{-1} yr^{-1}). In Southeast Asia, net losses were higher (20%), because here deforestation fires were more widely distributed within the ecosystem. In 'interior' tropical forests that were removed from the deforestation frontier (areas with fire emissions below a 500 kg C ha^{-1} yr^{-1} threshold), remote tropical fires led to a net gain of N by means of deposition. In interior forests in Africa, for example, the net atmospheric flux from fires was 0.50 Tg N yr^{-1} (3.4 kg N ha^{-1} yr^{-1}), corresponding to approximately 15% of BNF. In contrast, forests at the deforestation frontier in South America and Southeast Asia had a large net N loss at a regional scale from fire emissions. Expressed as a percentage of BNF, net N losses at the deforestation frontier (38%) were even higher than in savanna ecosystems.

Tropical oceans were a large recipient of N from fire emissions. Approximately 37% (2.85 Tg N yr^{-1}) of fire-emitted N_r was deposited over oceans. The tropical Atlantic, in particular, received high N deposition fluxes – up to 3.8 kg N ha^{-1} yr^{-1} (Fig. 3), owing to high levels of fire emissions in Africa and the prevalent easterly wind during the fire season (see Fig. S4). A small amount of the N from African fire emissions was transported across the Atlantic and deposited over South America. This pattern is consistent with analysis of lidar measurements from Manaus that show long-range transport of smoke and dust from Africa (Ansmann *et al.*, 2009). The southern part of South China Sea also received substantial N deposition (up to 2.7 kg N ha^{-1} yr^{-1}) from fires in Indonesia and Peninsular Malaysia.

Redistribution of N between ecosystems in Africa

Fires caused a net transport of N from savannas to interior forests in tropical Africa (Fig. 3 and Table 2). Evergreen broadleaf forests were distributed mostly between 5°N and 5°S and were bordered to the north and south by savannas (Fig. 6a). BNF was highest near the equator and decreased to the north and south with decreasing ET (Fig. 6b). The highest levels of N_r and N_2 fire emissions occurred at ~7°N in the NH and ~10°S in the southern hemisphere. The N deposition pattern, particularly for dry deposition, was similar to that of fire emissions but with a small equatorward shift in location of the peak deposition in the NH. A portion of N_r emitted from savanna fires was deposited back in savannas. However, a substantial amount of fire-emitted N_r was transported further equatorward and deposited in tropical forests. In NH winter, which corresponded to the NH fire season, prevailing winds

Table 2 N fluxes from fires (averaged over 1997–2006) in tropical regions

Continent	Region	Area (mHa)	Biological nitrogen fixation ($Tg\,N\,yr^{-1}$)	Fire emissions of N_r ($Tg\,N\,yr^{-1}$)	Fire emissions of N_2 ($Tg\,N\,yr^{-1}$)	Deposition of fire-emitted N		Net fire N flux	
						$Tg\,N\,yr^{-1}$	% of BNF	$Tg\,N\,yr^{-1}$	% of BNF
Africa	Tropical Forest*	287	6.56	0.67	0.69	1.19	18	−0.17	−3
(30°W–50°E;	Interior†	148	3.48	0.05	0.05	0.61	17	0.50	15
30°S–30°N)	Frontier‡	5	0.11	0.01	0.01	0.01	14	−0.01	−5
	Savanna§	1166	19.42	4.30	4.66	2.30	12	−6.66	−34
	Ocean	2966	20.29	0	0	1.21	6	1.21	6
South America	Tropical Forest	693	16.24	0.64	0.66	0.61	4	−0.70	−4
(80°W–30°W;	Interior	500	11.83	0.11	0.11	0.27	2	0.04	0
30°S–15°N)	Frontier	58	1.41	0.20	0.20	0.12	8	−0.29	−20
	Savanna	502	10.24	0.66	0.71	0.46	5	−0.91	−9
	Ocean	1494	10.22	0	0	0.28	3	0.28	3
Southeast Asia	Tropical Forest	301	8.05	1.16	1.05	0.59	7	−1.63	−20
(90°E–150°E;	Interior	90	2.35	0.03	0.03	0.09	4	0.03	1
20°S–20°N)	Frontier	46	1.23	0.46	0.47	0.22	18	−0.70	−57
	Savanna	141	2.79	0.37	0.37	0.15	5	−0.59	−21
	Ocean	2523	13.80	0	0	0.87	6	0.87	6
All tropics	Tropical Forest	1403	36.82	2.70	2.62	2.49	7	−2.83	−8
(180°W–180°E;	Interior	752	17.94	0.20	0.21	0.97	5	0.57	3
30°S–30°N)	Frontier	126	3.12	0.78	0.80	0.40	13	−1.18	−38
	Savanna	2085	38.83	5.49	5.91	3.02	8	−8.39	−22
	Ocean	19 530	120.11	0	0	2.85	2	2.85	2

The domains of tropical regions in Africa, South America, and Southeast Asia are shown in Fig. 3. MODIS-IGBP vegetation classes from the MODIS 500 m land cover product (MOD12) were used to determine biome types. Biological nitrogen fixation (BNF) rates were estimated using the mean of central and conservative regressions between BNF and evapotranspiration (ET) as given in Cleveland *et al*. (1999).

*'Tropical Forest' refers to 'evergreen broad leaf forest' in the MODIS-IGBP classification.

†'Interior' refers to tropical forest regions that are rarely affected by human activities. In this study, they are defined as $2^\circ \times 2.5^\circ$ grid cells where the fraction of evergreen broad leaf forest (from MODIS 500 m land cover product) is over 30% and the 10-year average fire emission rate (from GFEDv2) is smaller than $500\,kg\,C\,ha^{-1}\,yr^{-1}$.

‡'Frontier' refers to tropical forest regions undergoing substantial anthropogenic deforestation. Here they are defined as regions with forest cover >30% and with the fraction of forest loss during 2000–2005 (Hansen *et al*., 2008) >1%.

§'Savanna' includes 'savanna,' 'woody savanna,' and 'grassland' classes in the MODIS-IGBP classification.

MODIS, Moderate Resolution Imaging Spectroradiometer; GFEDv2, Global Fire Emissions Database version 2.

were to the south toward the Intertropical Convergence Zone (ITCZ) in the SH (Fig. 6c). Convective lifting of air masses near the equator increased precipitation and, subsequently, rates of wet deposition in tropical forests. The transport was reversed in NH summer, when winds to the north carried emissions from SH savannas across interior forests. The Sahara and Kalahari deserts, which were located upwind of the African savanna regions during the fire seasons in the northern and southern hemispheres, respectively, received relatively small N deposition fluxes from fire emissions.

The combined effects of biomass burning emissions, atmospheric transport, and deposition resulted in a net transport of N from savannas to forests in Africa (Figs 6f and 3c). This equatorward transport pattern was not unique to Africa. Prevailing winds in South America and Southeast Asia also caused transport of fire emissions toward interior (and relatively undisturbed) areas of the Amazon and the Indonesian archipelago (Fig. S4). This may be explained more generally by a covariance between fire emissions and relatively strong surface winds (toward the ITCZ) associated with the winter hemisphere of a Hadley cell (e.g., Plumb & Mahlman, 1987).

Discussion

Consequences for terrestrial ecosystem processes

In terms of assessing the impact of the N fluxes described above for tropical ecosystem functioning, it may be useful

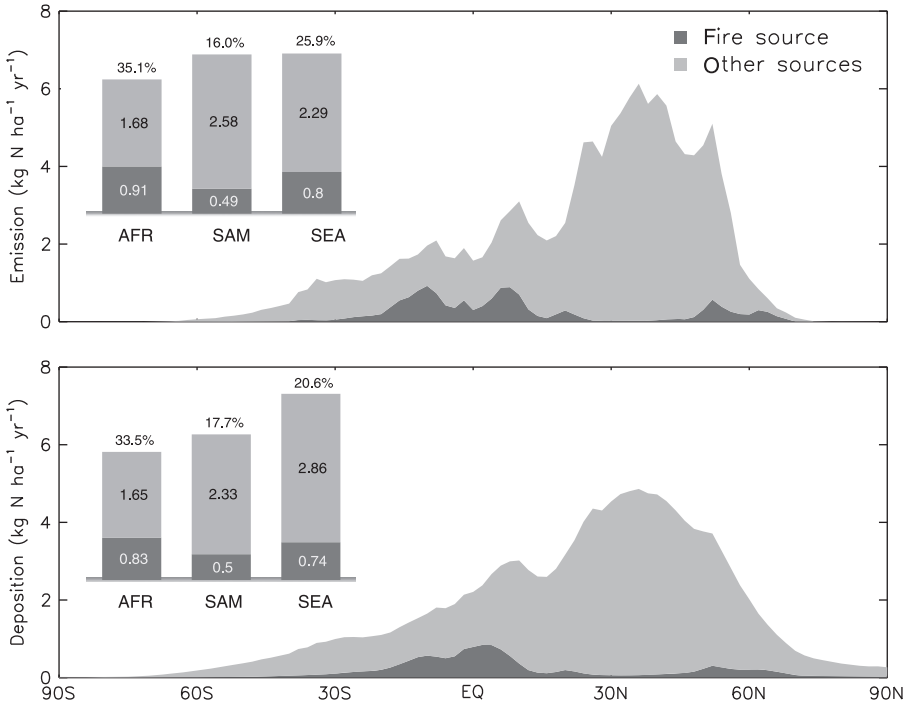

Fig. 4 Latitudinal distribution of reactive N (N_r) emission and deposition rates (kg N ha^{-1} yr^{-1}) from fires and other sources. Inserted plots show the mean values and fire contribution fractions for three tropical regions as defined in Fig. 3. The values are 10-year (1997–2006) averages.

to consider two timescales – one over the last millennium (but before the Industrial Revolution) and another covering the period after World War II when rates of tropical deforestation have been high (Houghton, 2003; Hurtt *et al*., 2006). Before the Industrial Revolution, humans had important roles in shaping the fire regime across South America, Africa, Australia, and Southeast Asia, particularly in savannas (e.g., Marlon *et al*., 2009). More recently, fire has been deployed at an unprecedented scale as a tool in clearing tropical forests and peatlands for pastures and croplands, often in conjunction with large-scale agricultural efforts (Page *et al*., 2002; DeFries *et al*., 2008; Langner & Siegert, 2009) and more extensively in South America and Southeast Asia than in Africa (e.g., Hansen *et al*., 2008). The fire emissions time series we used here contained components associated with human activities spanning both timescales.

Fires in savannas and at the deforestation frontier account for a substantial amount of global fire emissions. Fires in savannas were 1.2 Pg C yr^{-1} during 1997–2006, the most of any biome globally and accounting for 50% of global fire carbon emissions (van der Werf *et al*., 2006). In Africa, where most savannas are located, the impact of recent increases in population and concurrent changes in land use have not necessarily increased fire emissions (Archibald *et al*., 2009). Fire emissions at the deforestation frontier, defined here as fires in areas where humid tropical forest cover loss was measured using independent Landsat and MODIS observations (Hansen *et al*., 2008), were also substantial during 1997–2006, accounting for 30% of global fire emissions (0.7 Pg C yr^{-1}) (Le Quere *et al*., 2009). This latter component of global fire emissions is a relatively new phenomena and one that is directly linked with rates of forest and peatland clearing for pastures and crops (Morton *et al*., 2008; van der Werf *et al*., 2008). In South America, this component of fire emissions was distributed across the 'arc of deforestation' across Bolivia and Brazil (Schroeder *et al*., 2005). In Southeast Asia, these emissions were interspersed among forests across the Indonesian archipelago and other countries including Malaysia, Mynamar, Vietnam, and Thailand. Deforestation rates in Africa during 2000–2005 were much lower than in Asia or South America (Hansen *et al*., 2008), implying that the fire-emitted component of carbon losses associated with this flux were lower as well.

On millennial timescales, the cross-biome transport of N documented here may help to sustain productivity levels within tropical forests in central Africa, particularly given that this flux is accompanied in many areas by fine-mode black carbon aerosols containing phosphorus and potassium (Mahowald *et al*., 2005) and phosphorus from other natural sources (Mahowald *et al*., 2008). Although many soils in central Africa are oxisols and utisols (USDA-NRCS, 2005) where P would be expected to be the primary element limiting NPP, some studies suggest

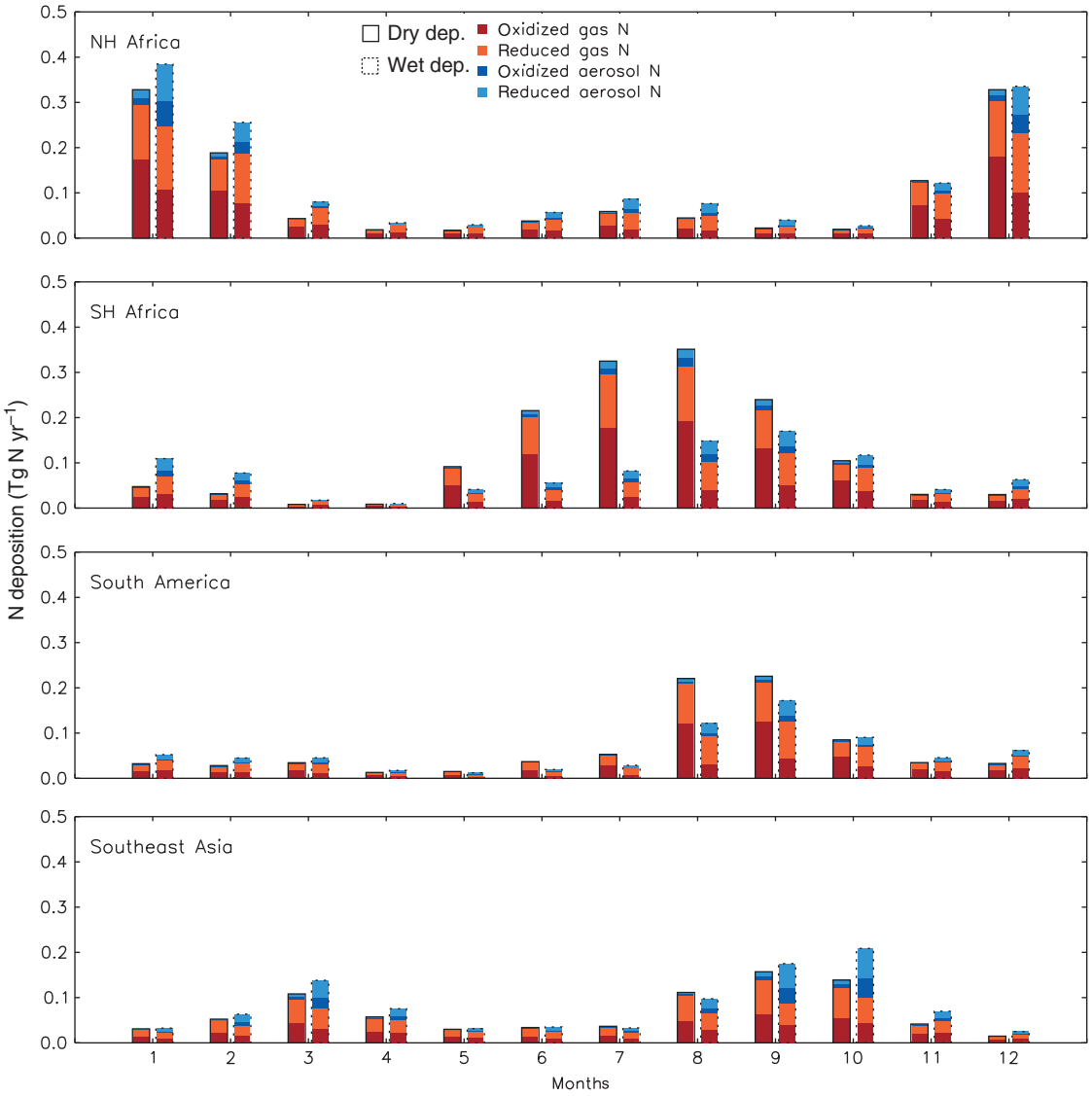

Fig. 5 Seasonal variability of total dry and wet deposition (Tg N yr^{-1}) of N from biomass burning over northern hemisphere (NH) Africa, Southern Hemisphere (SH) Africa, South America, and Southeast Asia (the domains are defined in Fig. 3). The values are the 10-year (1997–2006) mean from the GEOS-Chem simulation.

that even on highly weathered soils the effect of combined N and P additions can exceed that of P alone (Tanner *et al.*, 1992; Mirmanto *et al.* 1999; Harrington *et al.*, 2001; Campo & Vázquez-Yanes, 2004). Long-term N deposition fluxes from fires are likely to influence other ecosystem processes, including rates of decomposition in actively cycling soil carbon components and carbon storage in the bulk soil (e.g., Cusack *et al.*, 2009). For Africa, until better long-term records of fire activity become available, it remains difficult to assess unidirectional shifts in the fire regime and thus consequences for trends in NPP and carbon storage within tropical forests (e.g., Lewis *et al.*, 2009) by means of the atmospheric transport pathways assessed here.

In contrast with Africa, deforestation fires in South America and Southeast Asia have probably substantially modified N and P deposition rates in recent decades, particularly in areas near the deforestation frontier. On Borneo, for example, airport visibility records show marked increases in atmospheric aerosol concentration during El Nino events only after large-scale government efforts to increase settlements on the island occurred during the 1980s and 1990s (Field *et al.*, 2009). In the southern Amazon, long-term active fire records show increases in fire activity near transportation corridors (Schroeder *et al.* 2005) that have increased in spatial extent in recent decades. Secondary forest areas on these two continents are widespread and interspersed within areas

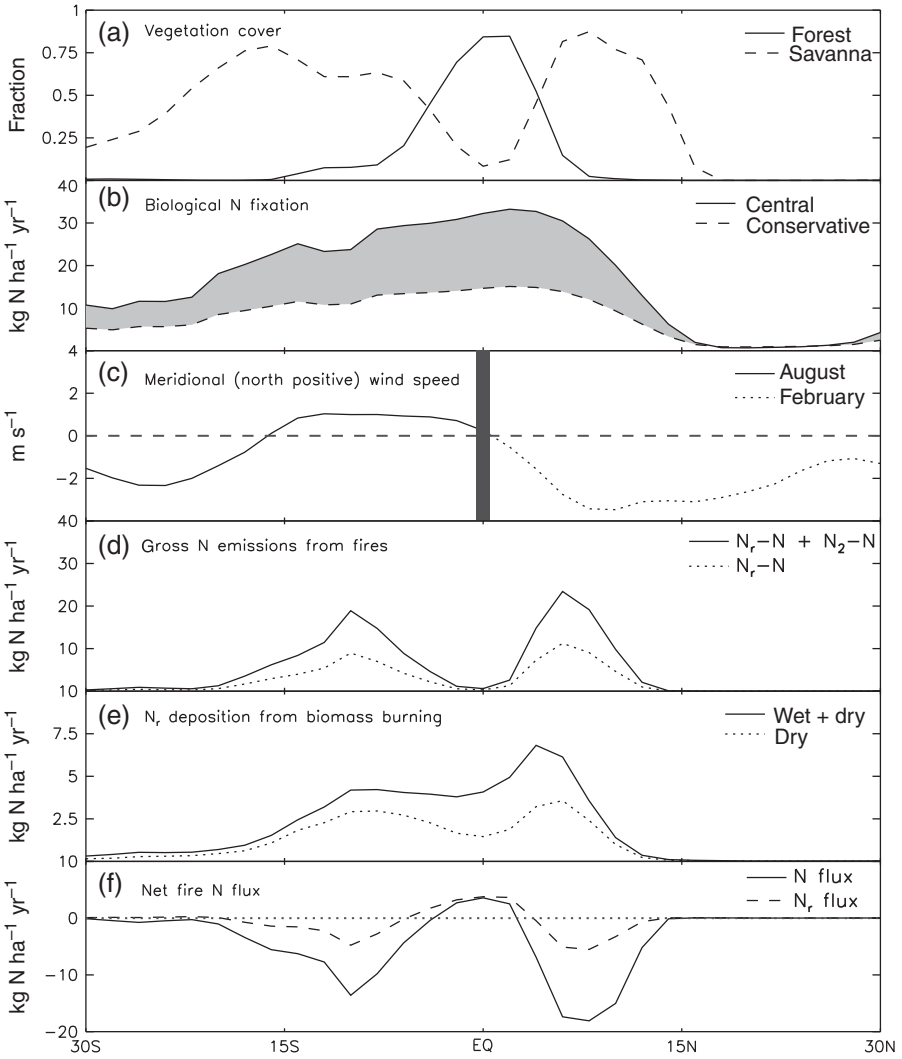

Fig. 6 Latitudinal distributions of mean (a) fraction of forest and savanna cover, (b) biological nitrogen (N) fixation (kg N ha^{-1} yr^{-1}) estimated from Cleveland *et al*. (1999), (c) meridional wind speed (m s^{-1}) at 850 hPa, with northward wind denoted as positive, (d) N emissions from fires, (e) N deposition from fires, and (f) net fire N and reactive N (N_r) fluxes (kg N ha^{-1} yr^{-1}) for a north–south swath across Africa between 10°E and 30°E. The net fire N_r flux includes losses from N_r emissions and gains from N_r deposition. This domain covers, from north to south, the Sahara desert, northern hemisphere (NH) savanna, tropical forest within the Congo Basin, southern hemisphere (SH) savanna, and the Karahari desert in Southwest Africa. The values are 10-year (1997–2006) averages. The meridional wind speed, derived from GEOS-4 reanalysis data, was averaged over February (during the time of peak fire activity in the NH) and August (during the time of peak fire activity in the NH).

of active deforestation (Hirsch *et al*., 2004; Hurtt *et al*., 2006). Multiple types of observations provide evidence for N limitation in these secondary forests (Campo & Vázquez-Yanes, 2004; Davidson *et al*., 2004; Davidson *et al*., 2007), suggesting they have the potential to respond to changes in deposition caused by fires.

The redistribution of N and P from deforestation fires may increase carbon storage in nearby primary and secondary forests in South America and Southeast Asia by stimulating NPP, and thus offsetting some of the net carbon loss associated with changes in carbon stocks in deforestation areas. These remote deposition-driven increases would likely be small in magnitude but widely distributed, thus serving potentially as one of the drivers for the observed increases in aboveground biomass measured over the last several decades in the Amazon (Philips *et al*., 2009). In the context of these atmospheric linkages, the amount of deforested biomass emitted as fire sets the relative importance of this negative feedback and highlights the need to improve our understanding of this highly uncertain component of the deforestation flux. Other fire effects on remote forests need to be considered in parallel, including increases in photosynthesis caused by aerosol effects on diffuse light

and canopy temperature (Oliveira *et al*., 2007; Mercado *et al*., 2009) as well as the deleterious effects of O_3 created by fire-emitted NO.

Deposition patterns associated with a changing fire regime will also likely interact with other drivers of global change. Modeling studies suggest tropical forests have great potential to increase NPP in response to elevated levels of CO_2 (Friedlingstein *et al*., 2006; Ciais *et al*., 2008), although a key uncertainty is whether nutrient availability can keep pace with photosynthesis to allow for long-term increases in biomass (e.g., Hungate *et al*., 2003; Luo *et al*., 2004; Thornton *et al*., 2009). Indeed, free air CO_2 enrichment studies from mid-latitude forests show that rates of carbon accumulation in response to elevated levels of CO_2 increase when nutrient availability is enhanced (Oren *et al*., 2001). If similar relationships exist for tropical secondary or primary forests, increasing deposition from deforestation fires may be enhancing the sensitivity of intact and recovering forests to increasing levels of atmospheric CO_2.

In other regions where N deposition rates are large from other sources, additional inputs from deforestation fires may have a negative effect on carbon storage by influencing nitrification and nitrate mobility in soil (e.g., Aber *et al*., 1998). We estimate that at present day, only 9.3% of the tropical forests have N deposition rate $>10\,\mathrm{kg\,N\,ha^{-1}\,yr^{-1}}$, a critical load over which the negative effect is evident (Dentener *et al*., 2006; Phoenix *et al*., 2006). However, Lamarque *et al*. (2005) suggest that a three-fold increase in N deposition over forested areas is possible from increasing fossil fuel combustion by 2100 compared with present-day conditions. Therefore, the combined influences of fire and energy production could increase the area of tropical forests receiving over $10\,\mathrm{kg\,N\,ha^{-1}\,yr^{-1}}$ in coming decades with potentially negative effects of N deposition occurring at these higher levels.

Consequences for ocean ecosystems

Detailed analysis of the effect of atmospheric N deposition on marine ecosystems is complex for several reasons. First, currently there are not enough observations to derive global maps of N fixation (Capone *et al*., 2005). Second, increases in atmospheric N deposition by anthropogenic activity may be partially offset by lower rates of N fixation (Krishnamurthy *et al*., 2007). Nevertheless, N is generally considered a primary limiting nutrient for phytoplankton biomass accumulation in marine ecosystems, particularly in coastal systems (Rabalais, 2002). A large portion (~37%) of N_r from savanna and forest fires is carried to and deposited over tropical oceans (Table 2). Averaged over the whole tropical ocean, this deposition is relatively small (2%) compared with BNF and also with respect to N transport to surface waters by upwelling (Capone *et al*., 2005). However, the ratio is much higher in coastal regions in Africa and Southeast Asia (Table 2) and the majority of the flux distributed in time over a period of only a few months. Further work is needed to identify how nutrient loading from fires affects marine ecosystem function in these highly impacted areas, including phytoplankton primary production and the health of coral reefs. In equatorial Asia after the 1997/1998 El Nino, for example, coral reef death was attributed to extraordinary red tide caused by deposition of iron from fire emissions (Abram *et al*., 2003).

Conclusions

We estimated the spatial patterns of emissions and deposition of N from tropical fires. Our results indicated a redistribution of N between different types of tropical ecosystems, with equatorward transport of N from fires in savannas and active deforestation frontiers to interior, tropical forests. On average, net fire losses were equivalent to 22% of BNF in savannas and 38% of BNF for ecosystems at the deforestation frontier. Interior tropical forests gained N equivalent to 3% of their BNF.

This atmospheric transport of N was closely related to the seasonality of fire emissions and meteorological patterns in tropics. The surface branch of the Hadley cell carried emissions from these fires toward the Intertropical Convergence Zone (ITCZ). In Africa, the prevailing winds carried fire emissions from savannas toward the Congo Basin during both NH and SH fire seasons. As a consequence of widespread savanna burning in Africa in both hemispheres, the net transfer of N from savannas to forests was larger than that observed in South America or Asia.

Improving our understanding of atmospheric N fluxes in tropical regions will require new measurement programs to collect key observations, including N deposition measurements near deforestation regions and improved estimates of N emissions from fires associated with forest clearing. More detailed measurements of N losses to N_2 during fires also are needed to reduce uncertainties associated with pyrodenitrification. Although considerable effort has gone into improving our understanding of the deposition of chemical species in tropics [e.g., the Deposition of Biogeochemically Important Trace Species (DEBITS) network, http://www.igac.noaa.gov/DEBITS.php], measurements of tropical N deposition are still sparse compared with the density of observations in available in temperate countries. Satellite measurements of NO_2 have the potential to provide important constraints in this regard, particularly with respect to emissions and some aspects of

chemistry and transport (e.g., Chai *et al*., 2009). In terms of assessing the impacts of a changing fire regime on carbon storage and species diversity, key uncertainties remain with respect to understanding interactions between deposition of N and other species such as P and potassium associated with fires and other natural and anthropogenic sources.

Acknowledgements

This work was supported by NASA Grant NNX08AF64G and NSF grant ATM0628353. P. Kasibhatla received additional support from NASA Grants NNX08AL03G and NNX08AQ04G to Duke University. The GEOS-Chem model was managed by the Atmospheric Chemistry Modeling group at Harvard University with support from the NASA Atmospheric Chemistry Modeling and Analysis Program.

References

Aber JD, McDowell WH, Nadelhoffer KG *et al*. (1998) Nitrogen saturation in temperate forest ecosystems: hypothesis revisited. *Bioscience*, **48**, 921–934.

Abram NJ, Gagan MK, McCulloch MT, Chappell J, Hantoro WS (2003) Coral reef death during the 1997 Indian Ocean dipole linked to Indonesian wildfires. *Science*, **301**, 952–955.

Andreae MO, Merlet P (2001) Emission of trace gases and aerosols from biomass burning. *Global Biogeochemical Cycles*, **15**, 955–966.

Ansmann A, Tesche M, Knippertz P, Bierwirth E, Althausen D, Muller D, Schulz O (2009) Vertical profiling of convective dust plumes in southern morocco during SAMUM. *Tellus Series B – Chemical and Physical Meteorology*, **61**, 340–353.

Archibald S, Roy DP, van Wilgen BW, Scholes RJ (2009) What limits fire? An examination of drivers of burnt area in Southern Africa. *Global Change Biology*, **15**, 613–630.

Atkinson R (2000) Atmospheric chemistry of VOCs and NOx. *Atmospheric Environment*, **34**, 2063–2101.

Bey I, Jacob DJ, Yantosca RM *et al*. (2001) Global modeling of tropospheric chemistry with assimilated meteorology: model description and evaluation. *Journal of Geophysical Research – Atmospheres*, **106**, 23073–23095.

Buis GM, Blair JM, Burkepile DE *et al*. (2009) Controls of aboveground net primary production in mesic savanna grasslands: an inter-hemispheric comparison. *Ecosystems*, **12**, 982–995.

Bustamante MMC, Medina E, Asner GP, Nardoto GB, Garcia-Montiel DC (2006) Nitrogen cycling in tropical and temperate savannas. Nitrogen cycling in tropical and temperate savannas. *Biogeochemistry*, **79**, 209–237.

Campo J, Vázques-Yanes C (2004) Effects of nutrient limitation on aboveground carbon dynamics during tropical dry forest regeneration in Yucatán, Mexico. *Ecosystems*, **7**, 311–319.

Capone DG, Burns JA, Montoya JP *et al*. (2005) Nitrogen fixation by *Trichodesmium* spp.: an important source of new nitrogen to the tropical and subtropical North Atlantic Ocean. *Global Biogeochemical Cycles*, **19**, GB2024, doi: 10.1029/2004GB002331.

Cech PG, Kuster T, Edwards PJ, Venterink HO (2008) Effects of herbivory, fire and N-2-fixation on nutrient limitation in a humid African savanna. *Ecosystems*, **11**, 991–1004.

Chai TF, Carmichael GR, Tang YH, Sandu A, Heckel A, Richter A, Burrows JP (2009) Regional NOx emission inversion through a four-dimensional variational approach using SCIAMACHY tropospheric NO2 column observations. *Atmospheric Environment*, **43**, 5046–5055.

Ciais P, Piao S-L, Cadule P, Friedlingstein P, Chedin A (2008) Variability and recent trends in the African carbon balance. *Biogeosciences Discussions*, **5**, 3497–3532.

Cleveland CC, Townsend AR, Schimel DS *et al*. (1999) Global patterns of terrestrial biological nitrogen (N-2) fixation in natural ecosystems. *Global Biogeochemical Cycles*, **13**, 623–645.

Cochrane MA, Alencar A, Schulze MD, Souza CM Jr., Nepstad DC, Lefebvre P, Davidson EA (1999) Positive feedbacks in the fire dynamic of closed canopy tropical forests. *Science*, **284**, 1832–1835.

Cook GD (1994) The fate of nutrients during fires in a tropical savanna. *Australian Journal of Ecology*, **19**, 359–365.

Crutzen PJ, Andreae MO (1990) Biomass burning in the tropics – impact on atmospheric chemistry and biogeochemical cycles. *Science*, **250**, 1669–1678.

Cusack DF, Torn MS, McDowell WH, Silver WL (2009) The response of heterotrophic activity and carbon cycling to nitrogen additions and warming in two tropical forest soils. *Global Change Biology*, doi: 10.1111/j.1365-2486.2009.02131.x.

Davidson EA, de Carvalho CJR, Figueira AM *et al*. (2007) Recuperation of nitrogen cycling in Amazonian forests following agricultural abandonment. *Nature*, **447**, 995–998.

Davidson EA, Reis de Carvalho CJ, Vieira IC *et al*. (2004) Nitrogen and phosphorus limitation of biomass growth in a tropical secondary forest. *Ecological Applications*, **14** (Supplement: LBA Experiment), 150–163.

Davidson EA, Nepstad DC, Ishida FY, Brando PM (2008) Effects of an experimental drought and recovery on soil emissions of carbon dioxide, methane, nitrous oxide, and nitric oxide in a moist tropical forest. *Global Change Biology*, **14**, 2582–2590.

de Graaf MCC, Bobbink R, Roelofs JGM, Verbeek PJM (1998) Differential effects of ammonium and nitrate on three heathland species. *Plant Ecology*, **135**, 185–196.

DeFries RS, Morton DC, van der Werf GR *et al*. (2008) Fire-related carbon emissions from land use transitions in southern Amazonia. *Geophysical Research Letters*, **35**, L22705, doi: 10.1029/2008GL035689.

Dentener F, Drevet J, Lamarque JF *et al*. (2006) Nitrogen and sulfur deposition on regional and global scales: a multimodel evaluation. *Global Biogeochemical Cycles*, **20**, GB4003, doi: 10.1029/2005GB002672.

Deutsch C, Gruber N, Key RM, Sarmiento JL, Ganachaud A (2001) Denitrification and N-2 fixation in the Pacific Ocean. *Global Biogeochemical Cycles*, **15**, 483–506.

Duce RA, LaRoche J, Altieri K *et al*. (2008) Impacts of atmospheric anthropogenic nitrogen on the open ocean. *Science*, **320**, 893–897.

Dunn PH, DeBano LF, Eberlein GE (1979) Effects of burning on chaparral soils: II. Effects of burning on chaparral soils: II. Soil microbes and nitrogen mineralization. *Soil Science Society of America Journal*, **43**, 509–514.

Elser JJ, Bracken MES, Cleland EE *et al*. (2007) Global analysis of nitrogen and phosphorus limitation of primary producers in freshwater, marine, and terrestrial ecosystems. *Ecology Letters*, **10**, 1135–1142.

Field CB, Behrenfeld MJ, Randerson JT, Falkowski P (1998) Primary production of the biosphere: integrating terrestrial and oceanic components. *Science*, **281**, 237–240.

Field RD, van der Werf GR, Shen SSP (2009) Human amplification of drought-induced biomass burning in Indonesia since 1960. *Nature Geosciences*, **2**, 185–188.

Fisher JB, Tu KP, Baldocchi DD (2008) Global estimates of the land-atmosphere water flux based on monthly AVHRR and ISLSCP-II data, validated at 16 FLUXNET sites. *Remote Sensing of Environment*, **112**, 901–919.

Friedlingstein P, Cox P, Betts R *et al*. (2006) Climate-carbon cycle feedback analysis: results from the (CMIP)-M-4 model intercomparison. *Journal of Climate*, **19**, 3337–3353.

Galloway JN, Aber JD, Erisman JW, Seitzinger SP, Howarth RW, Cowling EB, Cosby BJ (2003) The nitrogen cascade. *Bioscience*, **53**, 341–356.

Galloway JN, Dentener FJ, Capone DG *et al*. (2004) Nitrogen cycles: past, present, and future. *Biogeochemistry*, **70**, 153–226.

Galloway JN, Levy H, Kashibhatla PS (1994) Year 2020 – consequences of population-growth and development on deposition of oxidized nitrogen. *Ambio*, **23**, 120–123.

Galloway JN, Townsend AR, Erisman JW *et al*. (2008) Transformation of the nitrogen cycle: recent trends, questions, and potential solutions. *Science*, **320**, 889–892.

Giglio L, van der Werf GR, Randerson JT, Collatz GJ, Kasibhatla P (2006) Global estimation of burned area using MODIS active fire observations. *Atmospheric Chemistry and Physics*, **6**, 957–974.

Hansen MC, Stehman SV, Potapov PV *et al*. (2008) Humid tropical forest clearing from 2000 to 2005 quantified by using multitemporal and multiresolution remotely sensed data. *Proceedings of the National Academy of Sciences of the United States of America*, **105**, 9439–9444.

Harrington RA, Fownes JH, Vitousek PM (2001) Production and resource use efficiencies in N- and P-limited tropical forests: a comparison of responses to long-term fertilization. *Ecosystems*, **4**, 646–657.

Hirsch AI, Little WS, Houghton RA, Scott NA, White JD (2004) The net carbon flux due to deforestation and forest regrowth in the Brazilian Amazon: analysis using a process-based model. *Global Change Biology*, **10**, 908–924.

Hobbs NT, Schimel DS, Owensby CE, Ojima DS (1991) Fire and grazing in the tallgrass prairie: contingent effects on nitrogen budgets. *Ecology*, **72**, 1374–1382.

Hoffmann WA, Schroeder W, Jackson RB (2002) Positive feedbacks of fire, climate, and vegetation and the conversion of tropical savanna. *Geophysical Research Letters*, **29**, 2052, doi: 10.1029/2002GL015424.

Houghton RA (2003) Revised estimates of the annual net flux of carbon to the atmosphere from changes in land use and land management 1850–2000. *Tellus B*, **55**, 378–390.

Hungate BA, Dukes JS, Shaw MR, Luo YQ, Field CB (2003) Nitrogen and climate change. *Science*, **302**, 1512–1513.

Hurtt GC, Frolking S, Fearon MG *et al*. (2006) The underpinnings of land-use history: three centuries of global gridded land-use transitions, wood-harvest activity, and resulting secondary lands. *Global Change Biology*, **12**, 1208–1229.

Kaspari M, Garcia MN, Harms KE, Santana M, Wright SJ, Yavitt JB (2008) Multiple nutrients limit litterfall and decomposition in a tropical forest. *Ecology Letters*, **11**, 35–43.

Krishnamurthy A, Moore JK, Zender CS, Luo C (2007) Effects of atmospheric inorganic nitrogen deposition on ocean biogeochemistry. *Journal of Geophysical Research – Biogeosciences*, **112**, G02019, doi: 10.1029/2006JG000334.

Kuhlbusch TA, Lobert JM, Crutzen PJ, Warneck P (1991) Molecular nitrogen emissions from denitrification during biomass burning. *Nature*, **351**, 135–137.

Lamarque JF, Kiehl JT, Brasseur GP *et al*. (2005) Assessing future nitrogen deposition and carbon cycle feedback using a multimodel approach: analysis of nitrogen deposition. *Journal of Geophysical Research – Atmospheres*, **110**, D19303, doi: 10.1029/2005JD005825.

Langner A, Siegert F (2009) Spatiotemporal fire occurrence in Borneo over a period of 10 years. *Global Change Biology*, **15**, 48–62.

Le Quere C, Raupach MR, Ganadell JG *et al*. (2009) Trends in the sources and sinks of carbon dioxide. *Nature Geoscience*, 2009, doi: 10.1038/ngeo689.

LeBauer DS, Treseder KK (2008) Nitrogen limitation of net primary productivity in terrestrial ecosystems is globally distributed. *Ecology*, **89**, 371–379.

Lee K, Karl DM, Wanninkhof R, Zhang JZ (2002) Global estimates of net carbon production in the nitrate-depleted tropical and subtropical oceans. *Geophysical Research Letters*, **29**, 1907, doi: 10.1029/2001GL014198.

Lewis SL, Lopez-Gonzalez G, Sonke B *et al*. (2009) Increasing carbon storage in intact African tropical forests. *Nature*, **457**, 1003–1006.

Liu HY, Jacob DJ, Bey I, Yantosca RM (2001) Constraints from Pb-210 and Be-7 on wet deposition and transport in a global three-dimensional chemical tracer model driven by assimilated meteorological fields. *Journal of Geophysical Research – Atmospheres*, **106**, 12109–12128.

Lobert JM, Scharffe DH, Hao WM, Crutzen PJ (1990) Importance of biomass burning in the atmospheric budgets of nitrogen-containing gases. *Nature*, **346**, 552–554.

Luo Y, Su B, Currie WS *et al*. (2004) Progressive nitrogen limitation of ecosystem responses to rising atmospheric carbon dioxide. *Bioscience*, **54**, 731–739.

Mack MC, D'Antonio CM (1998) Impacts of biological invasions on disturbance regimes. *Trends in Ecology & Evolution*, **13**, 195–198.

Mack MC, D'Antonio CM, Ley RE (2001) Alteration of ecosystem nitrogen dynamics by exotic plants: a case study of C4 grasses in Hawaii. *Ecological Applications*, **11**, 1323–1335.

Mahaffey C, Michaels AF, Capone DG (2005) The conundrum of marine N-2 fixation. *American Journal of Science*, **305**, 546–595.

Mahowald N, Jickells TD, Baker AR *et al*. (2008) Global distribution of atmospheric phosphorus sources, concentrations and deposition rates, and anthropogenic impacts. *Global Biogeochemical Cycles*, **22**, GB4026, doi: 10.1029/2008GB003240.

Mahowald NM, Artaxo P, Baker AR, Jickells TD, Okin GS, Randerson JT, Townsend AR (2005) Impacts of biomass burning emissions and land use change on Amazonian atmospheric phosphorus cycling and deposition. *Global Biogeochemical Cycles*, **19**, GB4030, doi: 10.1029/2005GB002541.

Marlon JR, Bartlein PJ, Carcaillet C *et al*. (2009) Climate and human influences on global biomass burning over the past two millennia. *Nature Geosciences*, **2**, 307, doi: 10.1038/ngeo468.

Matson PA, McDowell WH, Townsend AR, Vitousek PM (1999) The globalization of N deposition: ecosystem consequences in tropical environments. *Biogeochemistry*, **46**, 67–83.

Mercado LM, Bellouin N, Sitch S, Boucher O, Huntingford C, Wild M, Cox PM (2009) Impact of changes in diffuse radiation on the global land carbon sink. *Nature*, **458**, 1014–1017.

Mirmanto E, Proctor J, Green J, Suriantata LN (1999) Effects of nitrogen and phosphorus fertilization in a lowland evergreen rainforest. *Philosophical Transactions of the Royal Society of London (Series B)*, **354**, 1825–1829.

Morton DC, deFries R, Randerson JT, Giglio L, Schroeder W, Van der Werf GR (2008) Agricultural intensification increases deforestation fire activity in Amazonia. *Global Change Biology*, **14**, 1–14.

Neff JC, Keller M, Holland EA, Weitz AW, Veldkamp E (1995) Fluxes of nitric oxide from soils following the clearing and burning of a secondary tropical rain forest. *Journal of Geophysical Research*, **100**, 25,913–25,922.

Novelli PC, Masarie KA, Lang PM (1998) Distributions and recent changes of carbon monoxide in the lower troposphere. *Journal of Geophysical Research–Atmosphere*, **103**, 19015–19033.

Okello BD, Young TP, Riginos C, Kelly D, O'Connor T (2008) Short-term survival and long-term mortality of *Acacia drepanolobium* after a controlled burn in Laikipia, Kenya. *African Journal of Ecology*, **46**, 395–401.

Oliveira PHF, Artaxo P, Pires C *et al*. (2007) The effects of biomass burning aerosols and clouds on the CO_2 flux in Amazonia. *Tellus Series B – Chemical And Physical Meteorology*, **59**, 338–349.

Oren R, Ellsworth DS, Johnsen KH *et al*. (2001) Soil fertility limits carbon sequestration by forest ecosystems in a CO_2-enriched atmosphere. *Nature*, **411**, 469–472.

Page SE, Siegert F, Rieley JO, Boehm HDV, Jaya A, Limin S (2002) The amount of carbon released from peat and forest fires in Indonesia during 1997. *Nature*, **420**, 61–65, doi: 10.1038/nature01131.

Paulissen M, van der Ven PJM, Dees AJ, Bobbink R (2004) Differential effects of nitrate and ammonium on three fen bryophyte species in relation to pollutant nitrogen input. *New Phytologist*, **164**, 451–458.

Philips OL, Aragao L, Lewis SL *et al*. (2009) Drought sensitivity of the Amazon rainforest. *Science*, **323**, 1344–1347.

Phoenix GK, Hicks WK, Cinderby S *et al*. (2006) Atmospheric nitrogen deposition in world biodiversity hotspots: the need for a greater global perspective in assessing N deposition impacts. *Global Change Biology*, **12**, 470–476.

Plumb RA, Mahlman JD (1987) The zonally averaged transport characteristics of the GFDL general circulation model. *Journal of Atmospheric Sciences*, **44**, 298–327.

Rabalais NN (2002) Nitrogen in aquatic ecosystems. *Ambio*, **31**, 102–112.

Raison RJ, Khanna PK, Woods PV (1985) Mechanisms of element transfer to the atmosphere during vegetation fires. *Canadian Journal of Forest Research*, **15**, 132–140.

Scholes RJ, Archer SR (1997) Tree-grass interactions in savannas. *Annual Review of Ecology and Systematics*, **28**, 517–544.

Schroeder W, Morisette JT, Csiszar I, Giglio L, Morton D, Justice C (2005) Characterizing vegetation fire dynamics in Brazil through multisatellite data: common trends and practical issues. *Earth Interactions*, **9** (Paper No. 13), 1–26.

Smil V (1999) Nitrogen in crop production: an account of global flows. *Global Biogeochemical Cycles*, **13**, 647–662.

Stephens BB, Gurney KR, Tans PP *et al*. (2007) Weak northern and strong tropical land carbon uptake from vertical profiles of atmospheric CO_2. *Science*, **316**, 1732–1735.

Tanner EVJ, Kapos V, Franco W (1992) Nitrogen and phosphorus fertilization effects on Venezuelan montane forest trunk growth and litterfall. *Ecology*, **73**, 78–86.

Thornton PE, Doney SC, Lindsay K *et al*. (2009) Carbon–nitrogen interactions regulate climate-carbon cycle feedbacks: results from an atmosphere-ocean general circulation model. *Biogeosciences*, **6**, 2099–2120.

USDA-NRCS (2005) *Global Soils Regions Map. Natural Resources Conservation Service, USDA*. Soil Survey Division, World Soil Resources, Washington, DC.

van den Berg LJL, Peters CJH, Ashmore MR, Roelofs JGM (2008) Reduced nitrogen has a greater effect than oxidised nitrogen on dry heathland vegetation. *Environmental Pollution*, **154**, 359–369.

van der Werf GR, Dempewolf J, Trigg SN *et al*. (2008) Climate regulation of fire emissions and deforestation in equatorial Asia. *Proceedings of the National Academy of Sciences of the United States of America*, **105**, 20350–20355.

van der Werf GR, Randerson JT, Collatz GJ *et al*. (2004) Continental-scale partitioning of fire emissions during the 1997 to 2001 El Niño/La Niña period. *Science*, **303**, 73–76.

van der Werf GR, Randerson JT, Giglio L, Collatz GJ, Kasibhatla PS, Arellano AF (2006) Interannual variability in global biomass burning emissions from 1997 to 2004. *Atmospheric Chemistry and Physics*, **6**, 3423–3441.

Verchot LV, Hutabarat L, Hairiah K, van Noordwijk M (2006) Nitrogen availability and soil N_2O emissions following conversion of forests to coffee in southern Sumatra. *Global Biogeochemical Cycles*, **20**, GB4008, doi: 10.1029/2005GB002469.

Vitousek PM, Aber JD, Howarth RW *et al*. (1997) Human alteration of the global nitrogen cycle: sources and consequences. *Ecological Applications*, **7**, 737–750.

Vitousek PM, Farrington H (1997) Nutrient limitation and soil development: experimental test of a biogeochemical theory. Nutrient limitation and soil development: experimental test of a biogeochemical theory. *Biogeochemistry*, **37**, 63–75.

Wang YH, Jacob DJ, Logan JA (1998) Global simulation of tropospheric O-3-NOx-hydrocarbon chemistry 1. Model formulation. *Journal of Geophysical Research – Atmospheres*, **103**, 10713–10725.

Xia J, Wan S (2008) Global response patterns of terrestrial plant species to nitrogen addition. *New Phytologist*, **179**, 428–439.

Yienger JJ, Levy H (1995) Empirical-model of global soil-biogenic nox emissions. *Journal of Geophysical Research-Atmospheres*, **100**, 11447–11464.

Supporting Information

Additional Supporting Information may be found in the online version of this article:

Figure S1. Time series of monthly mean CO anomalies from NOAA GMD stations and the GEOS-Chem model.
Figure S2. The fraction of N lost to N_2 during fire emissions as a function of the CO to CO_2 ratio.
Figure S3. Forest cover loss in tropical regions.
Figure S4. Biomass burning emissions and 850 kPa wind vectors for South America, Africa, and Southeast Asia.
Table S1. Summary of N deposition observations.
Table S2. N fluxes from fires in tropical regions – same as Table 2 but expressed in units of N emissions or deposition per unit of land area.

Please note: Wiley-Blackwell are not responsible for the content or functionality of any supporting materials supplied by the authors. Any queries (other than missing material) should be directed to the corresponding author for the article.